

# Measurement of silicon surface recombination velocity using ultrafast pump–probe reflectivity in the near infrared

A. J. Sabbah and D. M. Riffe<sup>a)</sup>

*Physics Department, Utah State University, Logan, Utah 84322-4415*

(Received 15 June 2000; accepted for publication 16 August 2000)

We demonstrate that ultrafast pump–probe reflectivity measurements from bulk Si samples using a Ti:sapphire femtosecond oscillator ( $\lambda=800$  nm) can be used to measure the Si surface recombination velocity. The technique is sensitive to recombination velocities greater than  $\sim 10^4$  cm s<sup>-1</sup>. © 2000 American Institute of Physics. [S0021-8979(00)05222-1]

Carrier dynamics in Si are predominantly governed by the bulk relaxation time  $\tau_B$ , the surface recombination velocity (SRV)  $S$ , and the carrier diffusivity  $D$ . In order to measure these parameters a number of purely optical techniques—photomodulated reflectivity (PMR),<sup>1</sup> free-carrier absorption (FCA),<sup>2–4</sup> microwave photoconductive decay ( $\mu$ PCD),<sup>5</sup> and photothermal radiometry (PTR)<sup>6</sup> have been developed. The latter three of these techniques, which measure the total number of excess carriers in the sample (generated, for example, by a pulsed or harmonically modulated pump laser) become increasingly less sensitive to the SRV as the SRV increases. This is easily seen by considering the upper limit ( $=d^2/\pi^2D$ ) of the SRV contribution to the effective (measured) relaxation rate, which is valid for  $S > 40D/d$ , where  $d$  is the thickness of the sample being measured.<sup>7</sup> For a typical Si wafer thickness  $d=0.05$  cm and a diffusivity of  $10$  cm<sup>2</sup> s<sup>-1</sup>, we have an upper limit on measurable SRVs of  $\sim 10^4$  cm s<sup>-1</sup>. For the PMR technique, the sensitivity to large SRVs is limited to a similar range by the typical modulation-frequency limit of  $\sim 10^6$  Hz. Experimentally, SRVs on Si surfaces range between 0.25 (Ref. 8) and the thermal velocity limit of  $\sim 10^7$  cm s<sup>-1</sup>. These largest SRVs have been inferred from ultrafast two-photon photoemission studies.<sup>9</sup> As a compliment to these four optical techniques, it is desirable to have an optical probe with good sensitivity to SRVs greater than  $10^4$  cm s<sup>-1</sup>.

Here we demonstrate that picosecond pump–probe reflectivity using a Ti:sapphire oscillator operating at a wavelength  $\lambda=800$  nm is a sensitive probe of large SRVs on Si. With this technique a pump pulse excites electrons from the valence to conduction band. Dynamics of the excited carriers are then followed by monitoring the time-dependent reflectivity of the sample using a much weaker probe pulse. The sensitivity to surface recombination using 800 nm light is due to the combination of a large excitation depth ( $=9.8$   $\mu$ m) of the pump pulse combined with a small effective probe depth ( $=17$  nm) of the probe pulse. The large excitation depth results in negligible contribution to the near-surface carrier dynamics from diffusion into the bulk (on a 100 ps time scale), while the small probe depth results in the reflectivity

signal being sensitive only to changes in the carrier density very near the surface. Thus, the technique is suitable for measuring the SRV at one surface of a macroscopically thick sample, such as a commercial wafer, in contrast to FCA,  $\mu$ PCD, and PTR, which are sensitive to the SRV at both surfaces of commercial wafers.

The pump-probe reflectivity measurements were carried out with 25 fs pulses from a Ti-sapphire oscillator.<sup>10</sup> Normally incident, chopper-modulated pump pulses (fluence  $f_p \approx 1.25$  mJ cm<sup>-2</sup>) result in an initially excited near-surface carrier density of  $\sim 3.5 \times 10^{18}$  cm<sup>-3</sup>. The phase-sensitive-detected probe beam signal, derived from 33 times weaker, time-delayed probe pulses, is proportional to  $\Delta R/R$  ( $R$  is the reflectivity), which is  $\sim 3 \times 10^{-4}$  immediately following excitation by the pump.

In Fig. 1(a) we show the time dependent reflectivity signal from several Si(100) samples (cut from commercially manufactured wafers of  $\sim 1$  mm thickness), which were chosen to illustrate a wide range of SRVs measurable with the present technique. Curve A was obtained from a  $p$ -type (0.036  $\Omega$  cm) Si(100) sample with the native oxide layer present on the surface, while curve B was obtained from the same sample after a 1 min etch in HF acid, which removes the oxide and terminates the Si surface dangling bonds with H atoms. Curve C was obtained from an  $n$ -type Si(100) sample (1.85  $\Omega$  cm), also after an HF etch. At present it is unknown as to why the two samples exhibit such different reflectivity signals after the HF etch, although it may be related to near-surface defects which impact the ability of the H atoms to saturate the Si surface dangling bonds. Variations in the SRV of HF dipped samples have been previously noted.<sup>4</sup> Nonetheless, it is clear that the decay in reflectivity is significantly altered as a result of surface processing and can thus be linked to the SRV. As evident in Fig. 1, the initial reflectivity drop is followed by recovery back toward (or even past, in the case of curve C) the prepump reflectivity value. As we show below, the recovery in reflectivity is directly related to the SRV, with curves (a), (b), and (c) characterized by average surface recombination velocities of  $2.7 \times 10^4$ ,  $2.4 \times 10^5$ , and  $1.15 \times 10^6$  cm s<sup>-1</sup>, respectively.

In order to analyze the reflectivity changes we adopt a model previously used by several researchers to describe the time-dependent optical properties of Si.<sup>11,12</sup> This model consists of one-dimensional coupled diffusion equations for the

<sup>a)</sup> Author to whom correspondence should be addressed; electronic mail: riffe@cc.usu.edu

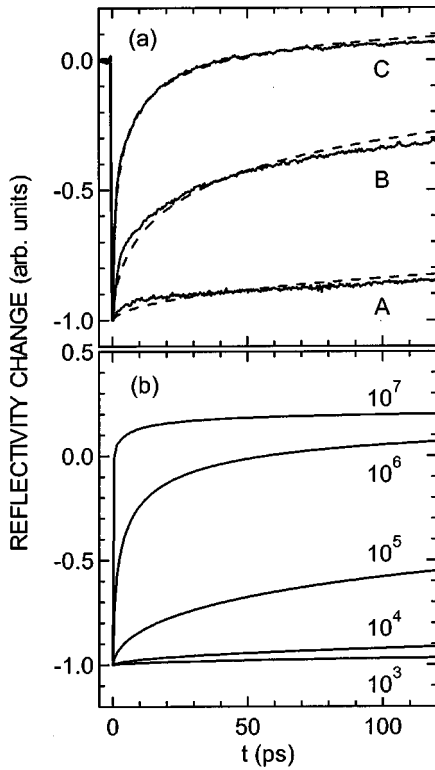


FIG. 1. Time dependence of the reflectivity. (a) Measured (solid) and calculated (dashed) reflectivity changes from three different Si surfaces. Calculated curves A, B, and C correspond to SRVs of  $2.7 \times 10^4$ ,  $2.4 \times 10^5$ , and  $1.15 \times 10^6$   $\text{cm s}^{-1}$ , respectively. (b) Calculated reflectivity changes for SRVs ranging from  $10^3$  to  $10^7$   $\text{cm s}^{-1}$ . The maximum change in reflectivity is normalized to  $-1$ .

excited carrier density  $N(z,t)$  and temperature  $T(z,t)$  (both of which affect the reflectivity as described below)

$$\frac{\partial N(z,t)}{\partial t} = \frac{\partial}{\partial z} \left[ D_N \frac{\partial N}{\partial z} \right] \quad (1)$$

and

$$\frac{\partial T(z,t)}{\partial t} = D_T \frac{\partial^2 T}{\partial z^2}, \quad (2)$$

where  $z$  is the distance from the Si surface,  $t$  is the time, and  $D_N$  is the ambipolar diffusivity, which depends on the free-carrier concentration,<sup>13</sup> and  $D_T = 0.88 \text{ cm}^2 \text{ s}^{-1}$  (Ref. 14) is the thermal diffusivity of Si.<sup>15</sup> In general, Eqs. (1) and (2) must also include bulk recombination terms.<sup>3</sup> However, on the time scale of 100 ps for an excitation density of  $3 \times 10^{18} \text{ cm}^{-3}$ , these bulk recombination processes are negligible in high-quality crystalline Si.<sup>16</sup> Equations (1) and (2) are coupled through the boundary conditions

$$SN(0,t) = D_N \left. \frac{\partial N}{\partial z} \right|_{z=0} = \frac{C}{E_g} D_T \left. \frac{\partial T}{\partial z} \right|_{z=0}, \quad (3)$$

where  $S$  is the SRV,  $E_g = 1.12 \text{ eV}$  is the band gap, and  $C = 1.64 \text{ J cm}^{-3} \text{ K}^{-1}$  the volume specific heat. The initial conditions  $N(z,0)$  and  $T(z,0)$  are given by

$$N(z,0) = \frac{C}{h\nu - E_g} [T(z,0) - T_L] = \frac{(1 - R_0)f_p}{h\nu\delta_1} \exp\left(\frac{-z}{\delta_1}\right), \quad (4)$$

where  $h\nu = 1.55 \text{ eV}$  is the photon energy,  $R_0 = 0.33$  is the normal-incidence reflectivity,  $T_L = 300 \text{ K}$  is the lattice temperature before arrival of the pump pulse, and  $\delta_1 = \lambda/4\pi k = 9.8 \mu\text{m}$  is the reciprocal of the attenuation coefficient. [Here  $k$  is the imaginary part of the complex index of refraction  $\hat{n} = n + ik = 3.695 + i0.0065$ .<sup>17</sup>] These initial conditions correspond to the state of the system immediately after thermalization of the excited carriers with the phonons, which occurs within a few hundred femtoseconds after excitation by the pump pulse.<sup>18</sup>

Equations (1)–(4) were numerically solved over the time scale of the experimental data shown in Fig. 1. The  $N$  dependence of  $D_N$  was taken to be that derived by Fletcher,  $D_N(N)^{-1} = D_0^{-1} + (N/A)\ln(1 + (B/N)^{2/3})$ . Here  $D_0 = 18 \text{ cm}^2 \text{ s}^{-1}$  is the low density limit of the diffusivity and  $A = 7 \times 10^{18} \text{ cm}^{-1} \text{ s}^{-1}$  and  $B = 0.54 \times 10^{18} \text{ cm}^{-3}$  were adjusted to match experimentally determined diffusivities.<sup>13</sup> Parts (a) and (b) of Fig. 2, respectively, show calculated values of  $N(z,t)$  and  $T(z,t)$  as a function of  $z$  for various delay times  $\Delta t = t$  between the pump and probe pulses for  $f_p = 1.25 \text{ mJ cm}^{-2}$  and  $S = 3 \times 10^5 \text{ cm s}^{-1}$ . As shown in Fig. 2 surface recombination depletes free carriers at the surface, which produces a sharp density gradient in the near-surface region. This density gradient produces net transport of carriers toward the surface, which continue to recombine there. Concurrently, the surface recombination produces a temperature rise at the surface, which diffuses into the Si.

Note that the relatively small attenuation coefficient [ $= (9.8 \mu\text{m})^{-1}$ ] for the pump pulse means that the initial density gradient is very small on the scale of the near-surface gradient produced by a SRV of  $3 \times 10^5 \text{ cm s}^{-1}$ . Hence, diffusion of carriers into the bulk on the time scale of the experiment is negligible and thus plays a minor role in the sub 100 ps near-surface dynamics. From Eqs. (3) and (4) it can be shown that the SRV induced gradient will be larger than the pump-pulse induced gradient for  $S > D_N/\delta_1 \approx 10^4 \text{ cm s}^{-1}$ . For  $S < 10^4 \text{ cm s}^{-1}$  diffusion into the bulk becomes as important as surface recombination in decreasing the carrier density in the near-surface region. Thus, recombination velocities greater than  $\sim 10^4 \text{ cm s}^{-1}$  can be determined.

The second factor that makes the technique sensitive to the SRV is the fact that the effective probe depth  $\delta_{\text{probe}} = \lambda/4\pi n = 17 \text{ nm}$  (Ref. 19) is very small on the length scale of the SRV induced gradient in  $N$ . Hence,  $\Delta R/R$  only depends on the carrier density at the surface. Thus, to calculate the time dependent reflectivity changes we need only consider  $N(0,t)$  and  $T(0,t)$ .

The dominant contribution to  $\Delta R/R$  is from  $N(0,t)$ , which produces a free-carrier intraband (Drude) term in the dielectric function  $\epsilon_D(N) = i(\omega_p(N)/\omega)^2 [\omega\tau/(1 - i\omega\tau)]$ . Here  $\omega_p^2(N) = 4\pi N e^2/m^*$  is the square of the plasma frequency, where  $e$  is the electron charge and  $m^* = 0.153m_e$  is the optical mass<sup>19</sup> ( $m_e$  is the electron mass);  $\omega$  is the laser frequency; and  $\tau \approx 100 \text{ fs}$  is the free-carrier scattering time.<sup>20</sup>

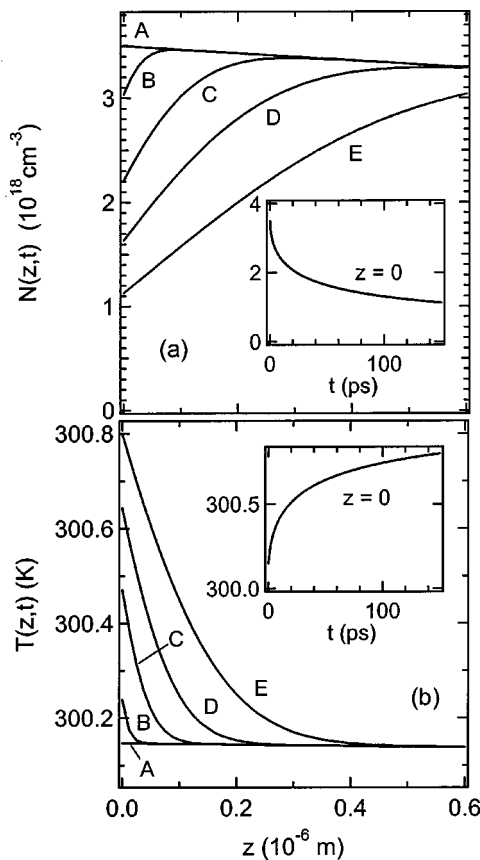


FIG. 2. Calculated values of  $N(z,t)$  and  $T(z,t)$ . (a) and (b), respectively, correspond to the  $z$  dependence of  $N(z,t)$  and  $T(z,t)$  for various time delay values  $t = \Delta t$ . Curves A, B, C, D, and E correspond to  $\Delta t$  equal to 0, 1.5, 15, 50, and 150 ps, respectively. Insets in (a) and (b), respectively, correspond to the  $t$  dependence of  $N(0,t)$  and  $T(0,t)$ .

The change in temperature also produces a change in optical constants. We model the temperature dependent change in optical constants using  $\partial n / \partial T = 3.4 \times 10^{-4} \text{ K}^{-1}$  (Ref. 21) and  $\partial k / \partial T = 3.5 \times 10^{-5} \text{ K}^{-1}$ .<sup>22</sup> In Fig. 1(b) we show calculated time-dependent reflectivity changes for  $S$  ranging from  $10^4$  to  $10^7 \text{ cm}^{-1}$ . Note that  $R$  increases with decreasing  $N$  and/or increasing  $T$ . Thus, for the largest values of  $S$  the  $T$  induced changes will dominate the  $N$  induced changes after the surface value of  $N$  has substantially decreased but before the temperature rise has significantly diffused into the bulk.

In Fig. 1(a) we display model curves that best fit the experimental data. Note that the only free parameter in the model is the SRV  $S$ . For all three curves that shape of the calculated curves matches the experimental data quite well, confirming that the SRV controls the near-surface carrier dynamics. However, (especially in curves A and B) the experimental data decay slightly faster at shorter times and more slowly at longer times than the model calculation. There are two likely explanations. The first is that  $S$  is time dependent on the picosecond time scale due to transient occupation effects of the surface states responsible for the recombination. The second possibility is that band bending effects (which

are not present in the model) may drive either the electrons or holes from the surface, thus decreasing surface recombination as a function of time. Both of these possibilities, which are currently being investigated, have been suggested from time-resolved photoemission measurements.<sup>23,24</sup>

In summary, we have demonstrated that carrier dynamics probed with real-time reflectivity on picosecond time scales by 800 nm radiation is a sensitive probe of surface recombination at Si surfaces. The technique is a useful bridge between slower optical techniques, which probe smaller SRVs and ultrafast photoemission techniques, which are more sensitive to occupied surface states rather than free carriers in the bulk.<sup>9,24</sup>

<sup>1</sup>J. Opsal and A. Rosenwaig, *Appl. Phys. Lett.* **47**, 498 (1985); C. Christofides, I. A. Vitkin, and A. Mandelis, *J. Appl. Phys.* **67**, 2815 (1990); **67**, 2822 (1990); A. Salnick, A. Mandelis, H. Ruda, and C. Jean, *ibid.* **82**, 1853 (1997).

<sup>2</sup>J. Waldmeyer, *J. Appl. Phys.* **63**, 1977 (1988); Z. G. Ling and P. K. Ajmera, *ibid.* **69**, 519 (1991); G. S. Kousik, Z. G. Ling, and P. K. Ajmera, *ibid.* **72**, 141 (1992); Z. G. Ling, P. K. Ajmera, and G. S. Kousik, *ibid.* **75**, 2718 (1994).

<sup>3</sup>J. Linnros, *J. Appl. Phys.* **84**, 275 (1998).

<sup>4</sup>J. Linnros, *J. Appl. Phys.* **84**, 284 (1998).

<sup>5</sup>M. Kunst, G. Müller, R. Schmidt, and H. Wetzel, *Appl. Phys. A: Solids Surf.* **46**, 77 (1988); A. Sanders and M. Kunst, *Solid-State Electron.* **34**, 1007 (1991); R. Schieck and M. Kunst, *ibid.* **41**, 1755 (1997); A. Buczkowski, Z. J. Radzinski, G. A. Rozgonyi, and F. Shimura, *J. Appl. Phys.* **72**, 2873 (1992).

<sup>6</sup>A. Salnick, A. Mandelis, and C. Jean, *Appl. Phys. Lett.* **69**, 2522 (1996); A. Mandelis, *Solid-State Electron.* **42**, 1 (1998).

<sup>7</sup>K. L. Luke and L.-J. Cheng, *J. Appl. Phys.* **61**, E282 (1987); A. B. Sproul, *ibid.* **76**, 2851 (1994); A. Schöneker, J. A. Eikelboom, A. R. Burgers, P. Lölgen, C. Leguijt, and W. C. Sinke, *ibid.* **79**, 1497 (1996).

<sup>8</sup>E. Yablonovitch, D. L. Allara, C. C. Chang, T. Gmitter, and T. B. Bright, *Phys. Rev. Lett.* **57**, 249 (1986).

<sup>9</sup>M. W. Rowe, H. Liu, G. P. Williams, and R. T. Williams, *Phys. Rev. B* **47**, 2048 (1993).

<sup>10</sup>M. T. Asaki, C.-P. Huang, D. Garvey, J. Zhou, H. C. Kapteyn, and M. M. Murnane, *Opt. Lett.* **18**, 977 (1993); D. M. Riffe and A. J. Sabbah, *Rev. Sci. Instrum.* **69**, 3099 (1998).

<sup>11</sup>M. G. Grimaldi, P. Baeri, and E. Rimini, *Appl. Phys. A: Solids Surf.* **33**, 107 (1984); O. B. Wright and V. E. Gusev, *Appl. Phys. Lett.* **66**, 1190 (1995).

<sup>12</sup>T. Tanaka, A. Harata, and T. Sawada, *J. Appl. Phys.* **82**, 4033 (1997).

<sup>13</sup>C.-M. Li, T. Sjödin, and H.-L. Dai, *Phys. Rev. B* **56**, 15252 (1997).

<sup>14</sup>Landolt-Bornstein, *Numerical Data and Functional Relationships in Science and Technology*, New Series, Group III, edited by O. Madelung, M. Schulz, and H. Weiss (Springer, Berlin, 1982), Vol. 17, Subvolume a.

<sup>15</sup>On a 100 ps time scale the density and temperature gradients of importance are generated within  $1 \mu\text{m}$  of the surface. Since this is much smaller than the lateral spot size or penetration depth of the pump, a one dimensional theory is appropriate.

<sup>16</sup>Raman spectra obtained from the samples were indicative of high-quality crystalline Si. M. Holtz (unpublished).

<sup>17</sup>D. E. Aspnes and A. A. Studna, *Phys. Rev. B* **27**, 985 (1983).

<sup>18</sup>See, e.g., T. Sjödin, H. Petek, and H.-L. Dai, *Phys. Rev. Lett.* **81**, 5664 (1998).

<sup>19</sup>H. M. van Driel, *Phys. Rev. B* **35**, 8166 (1987).

<sup>20</sup>E. Constant, in *Hot-Electron Transport in Semiconductors*, edited by L. Reggiani (Springer, New York, 1985), p. 233.

<sup>21</sup>G. E. Jellison and H. H. Burke, *J. Appl. Phys.* **60**, 841 (1986).

<sup>22</sup>H. M. van Driel, in *Semiconductors Probed by Ultrafast Laser Spectroscopy*, edited by R. R. Alfano (Academic, New York, 1984), Vol. II, p. 68.

<sup>23</sup>N. J. Halas and J. Bokor, *Phys. Rev. Lett.* **62**, 1679 (1989).

<sup>24</sup>S. Jeong and J. Bokor, *Phys. Rev. B* **59**, 4943 (1999).